On analysis of deformation and damage mechanisms of DYNEEMA composite under ballistic impact

L. Gilson, A. Imad, L. Rabet, F. Coghe

On analysis of deformation and damage mechanisms of DYNEEMA® composite under ballistic impact

L. Gilson[a,b], A. Imad[b,*], L. Rabet[a], F. Coghe[a]

[a] Royal Military Academy (RMA), 1000 Brussels, Belgium

[b] Univ. Lille, ULR 7512 – UML - Unité de Mécanique de Lille, Joseph Boussinesq, 59000 Lille, France

*Corresponding author: abdellatif.imad@polytech-lille.fr

Abstract. This paper deals with the assessment of damages occurred to an Ultra-High Molecular Weight Polyethylene (UHMWPE) based composite during ballistic impacts with two bi-metallic projectiles of different morphologies and masses. More specifically, the evaluated composite is DYNEEMA® HB80. The conditions of impact aim at evaluating the behind armour blunt trauma effects (BABT) of blocks of ballistic gelatine covered by the composite protection. The evaluated cases correspond to non-perforating impacts of the composite. The microstructure of the intact composite is precisely described. The damaged plates are compared to evaluate the influence of the projectile nature and to verify the influence of their kinetic energy on the displacement, deformations and damage mechanisms of the composite plate. Post-mortem analyses of the composite with incrusted projectiles are performed. Also, because the dynamic interaction process between the projectiles and armour plates was not visible, numerical simulations were conducted with LS-DYNA®. Overall, a good correlation was obtained between the tests and the models. An evaluation of the kinetic energy dissipation was also performed.

Keywords: composite protection, ballistic impact, damage mechanisms, projectile morphology, numerical simulations

1. Introduction

In the field of studies on the interaction between a projectile and a ballistic protection, the evaluation of the influence of projectiles parameters, like their morphology, already represents a research focus [1]. The nature of the target material also influences the interaction with the projectile.

In efforts to make ballistic protections lighter and more comfortable, new fibre-based products were developed. Most commonly, soft body armours are composed of high-performance fibre-based materials [2]. Typically, ultra-high molecular weight polyethylene (UHMWPE) fibres being produced by gel-spinning process [3-5] are considered as the strongest and lightest available fibres [4,6]. The low density but high elastic modulus in the fibre direction allows this type of material to quickly spread away the strain waves, thus the kinetic energy, associated with an impact process [7-9]. Based on various fabrics architectures, composite materials or laminates can be developed. For

example, Zhang et al. [10] compared the ballistic performance of laminates based on UHMWPE fabric with UD, 2D and 3D architectures. The authors observed the best performances with the UD construction in terms of impact velocity and kinetic energy absorption. Also, delamination is strongly more prevalent with the UD based construction than with the two others.

Most of the proposed works on UHMWPE composites concern the DYNEEMA® HB26 construction [3,5,6,11-15] produced by DSM. This laminate has a density of 970-980 g/m³ and is constituted of orthogonal layers of UD structured SK76 fibres associated to a polyurethane matrix occupying no more than 20% of the composite volume [4,12]. The SK76 fibres have diameters in the range of 17 ± 1 μm [3,16].

To study the microstructure of composite materials or more precisely assess the damage mechanisms of post-mortem samples, the most common imaging methods are dark field optical microscopy [6,13], scanning electron microscopy (SEM) [3] or X-ray computed tomography [3,12,17].

In efforts to get information about the damage process during the dynamic interaction between a projectile and the composite, numerical simulations are very often carried out. To assess the damages with such a model, fibre breaking, delamination, elastic and permanent deformation have to be taken into account [18]. A macroscopic representation of the composite is often used because it is sufficiently relevant to assess the main damage mechanisms for a reasonable computational cost [14,15,18]. In such an approach, the composite laminate is modelled by taking into account its thin sub-layers whose adhesion can be simulated with specific "tiebreak" contact algorithms including the normal and shear failure strengths [14,15,19,20]. The working principle of such an algorithm is reminded by Gilson et al. [20]. Only the damages at the yarn or filament level can not be predicted at this scale. For this, heavier simulations at the meso-/micro-scale levels can also be performed. Nevertheless, Chocron et al. [18] proved that simulations at both scales can provide quite similar global results (projectile deceleration during penetration) but in shorter delays.

It can be noted that only a few studies discussed and allow estimating the properties of DYNEEMA® HB80 construction [16-18,21-23]. The latter is quite similar to the HB26 one. It is composed of layers having the following architecture: 0°/90°/0°/90°. Each sub-layer contains about 2.5 SK76 filaments through the thickness. The single ply has an areal density of 0.145 kg/m² [16,18].

Chocron et al. [16] observed that the presence of the polyurethane matrix does not modify significantly the wave speed propagation into DYNEEMA® HB80 laminate during an impact. However, a flash occurs at the beginning of impact under the projectile, when it reaches the target, probably due to an auto-ignition of the composite related to the shock wave generated by the impact.

Zhang et al. [17,23] experimentally and numerically evaluate the influence of boundary conditions on the backface deformation (BFD) of DYNEEMA® HB80 plates. Apparently, this parameter is not responsible for a great effect on the BFD.

In previous studies, blocks of ballistic gelatine, unprotected [24,25] or covered with DYNEEMA® HB80 based ballistic protection [20,25] were impacted by two different deformable bi-metallic projectiles, having different morphologies and kinetic energies. In the first situation, perforation of the gelatine blocks allowed the selection and further validation of a specific material model for the gelatine. Covered with the ballistic protection, a complete experimental and numerical assessment of the behind armour blunt trauma (BABT) effect was performed.

In the present work, the structure of the composite and damages following the impact are evaluated in further details. Post-mortem analyses are performed with optical microscopy. As the post-mortem analysis of the plates does not give access to the damage processes of the composite, numerical simulations performed in the frame of our previous study [20,25] are investigated thoroughly. The continuous kinetic energy absorption is assessed to better understand how the composite defeats the projectiles.

2. Composite plates: materials and modelling

2.1. Materials and experimental procedure

The DYNEEMA® HB80 plates tested in a previous study [20] need to be described with more details. The square plates have a length of 200 mm. These laminates have a 5 mm thickness (Fig. 1(a)) and are composed of 34 plies, schematically detailed in Fig. 1(b). The real thickness of the single ply should be situated around 0.147 mm to give a composite with a 5 mm thickness.

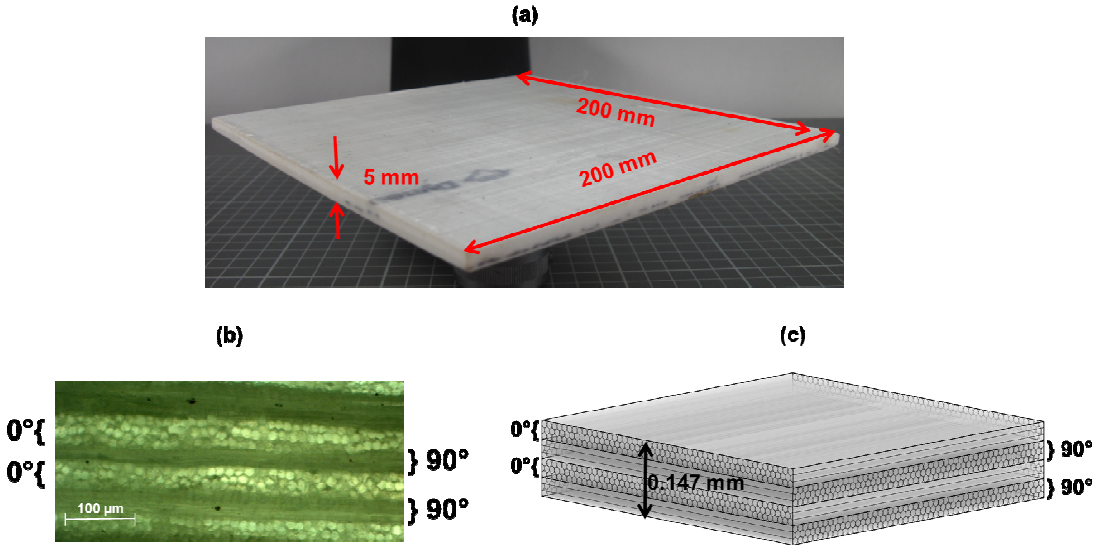

Fig. 1. *(a) Global view of the plate, (b) cross-section details of the composite plate and (c) schematic description of a single ply*

Such a composite has an orthotropic structure, obtained by compression and curing of the plies. Each ply is constituted of four sub-layers of UHMWPE filaments SK76 oriented in the direction 0°/90°/0°/90° (Fig. 1(b) and (c)) and associated to a polyurethane matrix. Nevertheless, it is apparently impossible to distinguish the interfaces between the plies from the interfaces between the sub-layers constituting the plies in the whole laminate. Moreover, if information exists about the inter-plies normal and shear resistance [20, 22], no data are available concerning the mechanical behaviour of the interfaces between the sub-layers. However, it can be noted that Lässig et al. [5,11,13] observed that higher consolidation (curing) pressures increase the performance of the armour plate. Thus, the mechanical response of these various interfaces (at least the inter-plies ones) can probably be modified by the making process (compression, heating and curing) of the composite.

The complete ballistic test setup is detailed in a previous study [20]. A pyrotechnic launcher placed at 5 meters from the composite plate to be impacted aimed at accelerating the projectiles. A Weibel® Doppler radar with 0.2% accuracy allowed measuring the projectiles velocities at impact. Their average values were respectively 390.25 m/s (Projectile 1) and 424.58 m/s (Projectile 2). These values are used as initial conditions for the simulations. It corresponds to impact kinetic energies of 605.37 J (Projectile 1) and 1402.49 J (Projectile 2). It can be noted that Projectile 2 has about 2.3 times the kinetic energy of Projectile 1.

2.2. Numerical modelling

Since suitable models of ballistic impact processes implicating DYNEEMA® products can be already performed at macroscopic scale [18], such an approach is considered in the present work based on the available information about DYNEEMA® HB80. Because the composite is constituted of 34 very thin plies, each of them is individually modelled as a single layer and meshed (Fig. 2(a)) with shell elements (Belytschko-Tsay shell formulation with 4 nodes) whose artificial thicknesses are 0.147 mm [20]. Consequently, the 4 sub-layers of each ply are homogenised as a single layer. Indeed, the shell formulation and the homogenisation of the sub-layers allow simplifying the calculations by reducing the number of elements and nodes of the model. Moreover, for a proper representation of the whole laminate composed of shell based layers, gaps of 0.147 mm are introduced between each modelled plies (Fig. 2(b) and (c)). Finally, the adhesion between the plies was defined by a suitable tiebreak contact algorithm taking into account the normal (Fig. 2(c)) and shear failure strength, whose values are respectively 15 and 60 MPa [20]. Such a contact algorithm allows modelling the delamination between the plies constituting the composite when a failure criterion is reached [20].

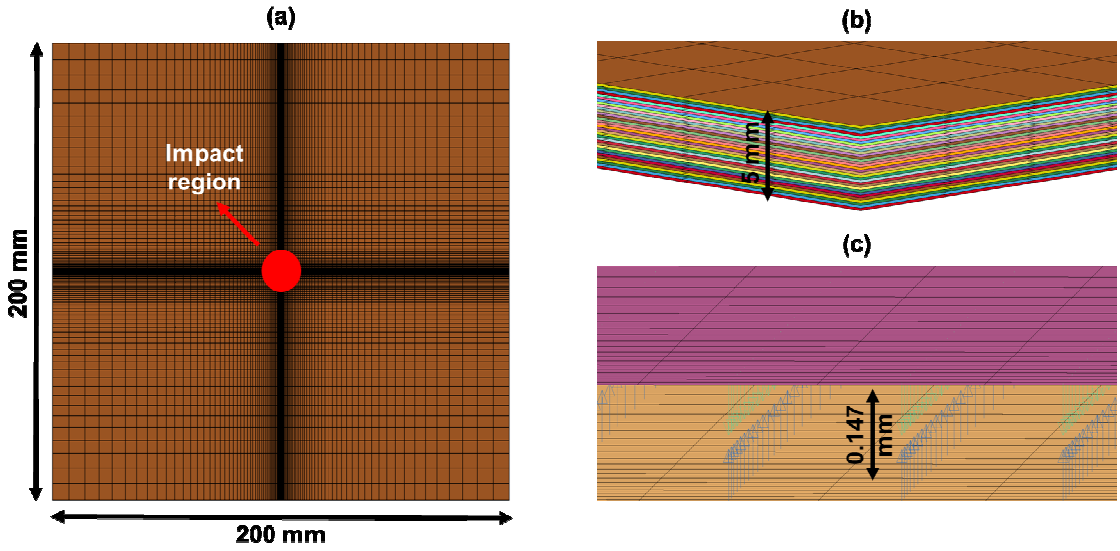

Fig. 2. Composite model. (a) Top view with refined mesh at the impact region, (b) cross-section view of the 34 plies and (c) two adjacent plies with interlaminate gap and vectors indicating the normal forces defining the contact

There is very few information concerning the mechanical behaviour of DYNEEMA® HB80. Available values are mainly based on elastic properties estimated from tensile tests results [21,22]. Thus, the orthotropic behaviour of the plate was introduced with a simplified orthotropic elastic model as a first approximation. The formulation of such a model is the following [19]:

$$C = T^T C_L T \qquad (1)$$

T is the transformation matrix and C_L is the constitutive matrix defined by:

$$C_L^{-1} = \begin{bmatrix} \frac{1}{E_a} & -\frac{\nu_{ba}}{E_b} & -\frac{\nu_{ca}}{E_c} & 0 & 0 & 0 \\ -\frac{\nu_{ab}}{E_a} & \frac{1}{E_b} & -\frac{\nu_{cb}}{E_c} & 0 & 0 & 0 \\ -\frac{\nu_{ac}}{E_a} & -\frac{\nu_{bc}}{E_b} & \frac{1}{E_c} & 0 & 0 & 0 \\ 0 & 0 & 0 & \frac{1}{G_{ab}} & 0 & 0 \\ 0 & 0 & 0 & 0 & \frac{1}{G_{bc}} & 0 \\ 0 & 0 & 0 & 0 & 0 & \frac{1}{G_{ca}} \end{bmatrix} \qquad (2)$$

$$\text{with } \frac{\nu_{ab}}{E_a} = \frac{\nu_{ba}}{E_b}, \frac{\nu_{ca}}{E_c} = \frac{\nu_{ac}}{E_a}, \frac{\nu_{cb}}{E_c} = \frac{\nu_{bc}}{E_b} \qquad (3)$$

where a, b and c define the main directions of the orthotropic composite, E is the Young modulus and ν is the Poisson ratio in the different main directions. Finally, the parameters associated with the mechanical behaviour of the DYNEEMA® HB80 are presented in Table 1. Also, a failure criterion (numerical erosion) was added to model penetration and perforation of composite layers based on a stress at failure of the ply set at 3 GPa [20,22,25].

Table 1. Material model parameters for DYNEEMA® HB80 [20,22,25]

ρ [kg/m³]	980
E_a [GPa]	5.99
$E_b = E_c$ [GPa]	56.32
$\nu_{ba} = \nu_{ca}$	0.5183
ν_{cb}	0.0269
G_{bc} [GPa]	0.89
$G_{ab} = G_{ca}$ [GPa]	0.4

3. Results and discussion

In this section, a presentation of the assessment of the global deformations and damage mechanisms of the composite plates and kinetic energy dissipation processes is performed.

3.1 Velocity decay, kinetic energy dissipation and dynamic processes

The numerical simulations allow the assessment of the continuous interaction between both objects. Indeed, from Fig. 3, it could be observed that Projectile 2 penetrates and displaces the composite deeper than Projectile 1.

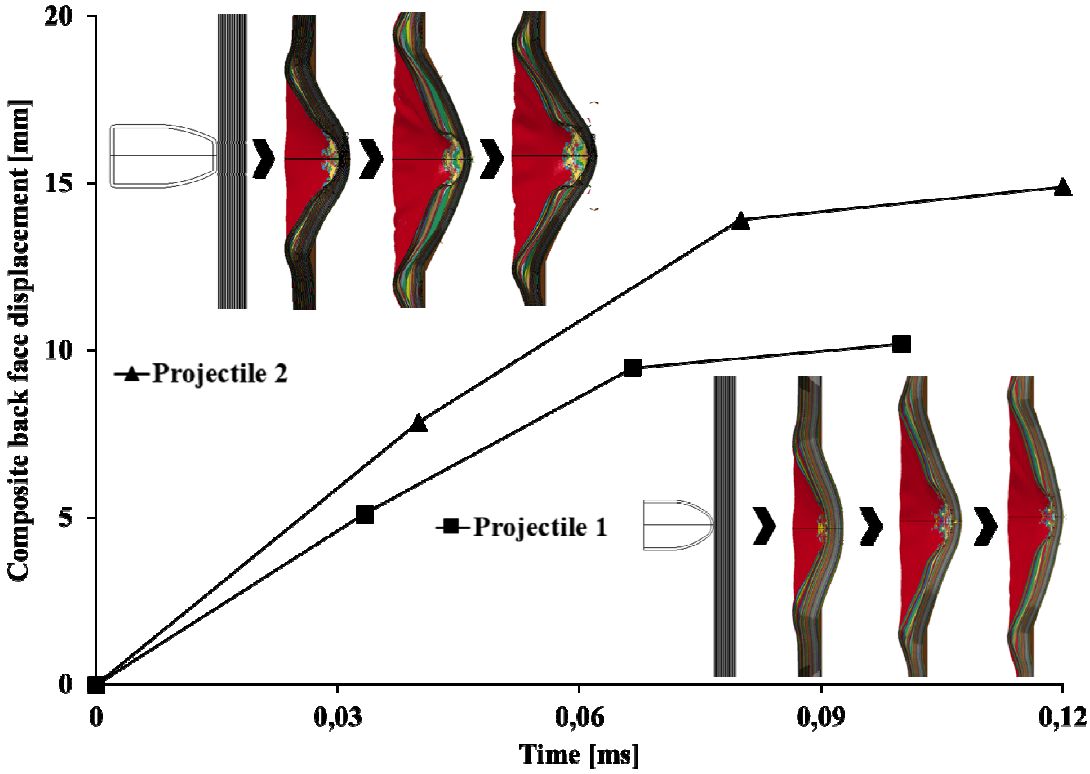

Fig. 3. *Numerical assessment of the deformation with time of the rear surface of the composite*

Also, as can be observed in Fig. 4, the deceleration curves of both projectiles are almost parallel. Thus, it can be supposed that with the same velocity as Projectile 2, both projectiles would decelerate similarly. It could mean that the deceleration of the projectiles is mainly governed by their momentum.

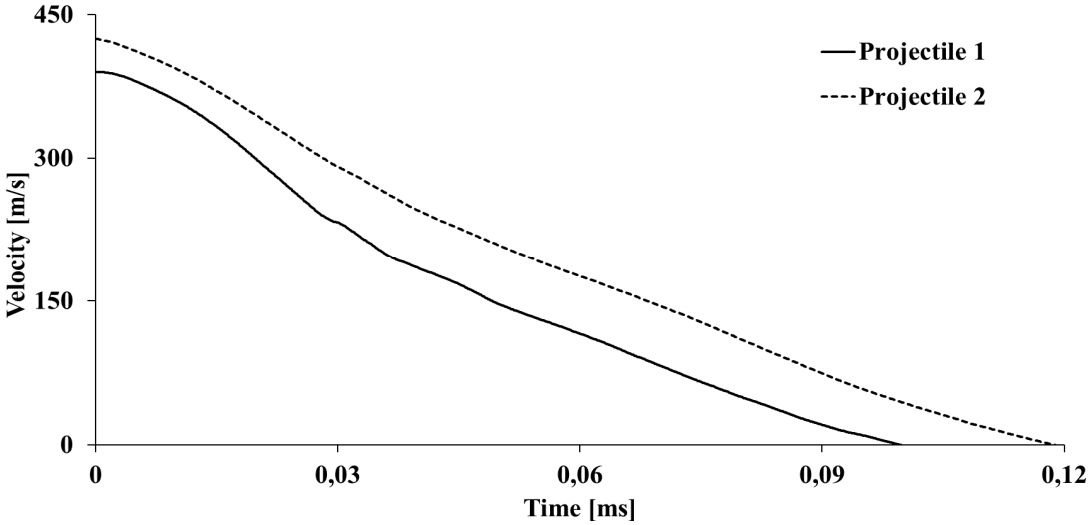

Fig. 4. *Velocity vs. time for projectiles 1 and 2*

It is important to note that the ballistic performance of a composite protection can be evaluated by energy absorption E_a, which can be determined from the following equation:

$$E_a = \frac{1}{2} m\left(V_i^2 - V_r^2\right) \qquad (4)$$

where m is the mass of the projectile (for Projectile 1, m_1 = 7.95 g and for Projectile 2, m_2 = 15.56 g), V_i and V_r are the impact and residual velocities of the projectile, respectively. In the present case, the impact is non-perforating. Thus, V_r = 0 m/s. Therefore, the energy absorbed by the composite plate is considered to be approximately equivalent to the impact kinetic energy (an undetermined part of this energy is also transformed into projectile deformation and, probably, into heat). Thus, for a given impact velocity, Projectile 2 has twice as much the kinetic energy as Projectile 1. The evolution of the kinetic energy with time of both projectiles (Thus, transmitted to the composite plate) is presented in Fig. 5. It can be noted that the plate absorbs a greater flow of energy in a shorter time with Projectile 2 than with Projectile 1.

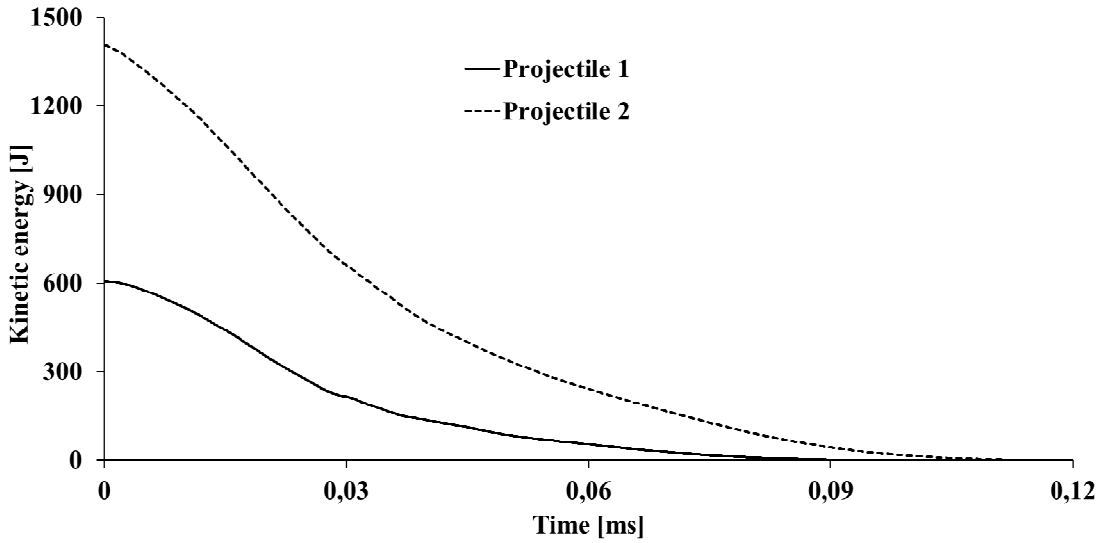

Fig. 5. *Numerical assessment of the evolution of the kinetic energy with time of both projectiles interacting with the composite*

Finally, as the composite is orthotropic, the main mechanism of kinetic energy dissipation is based on tensile solicitations of the UHMWPE fibres in the main directions as can be numerically assessed (Fig. 6). It indicates that the energy of the projectile is spread by deformations of the composite in its main directions firstly, and secondly on almost the whole surface of the composite. Of course, the effect is clearly more important in the case of Projectile 2.

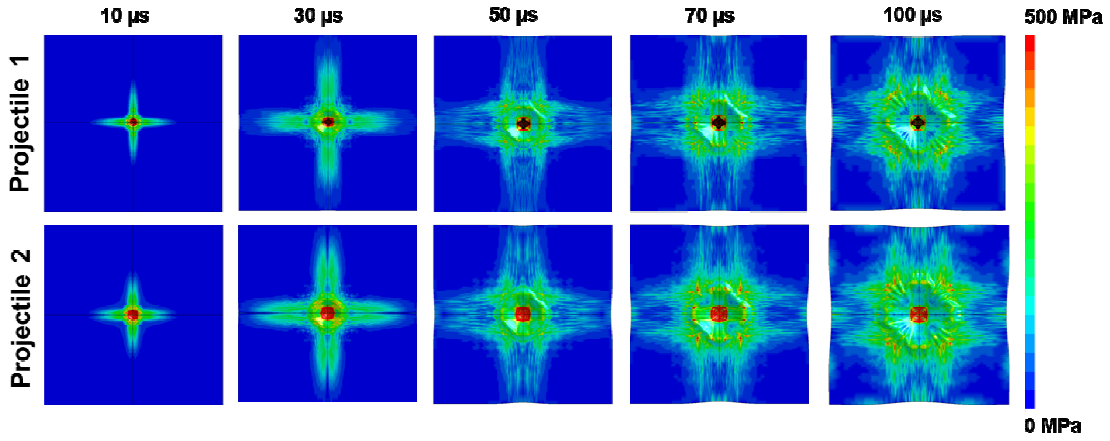

Fig. 6. *Numerical assessment of the tensile stress distribution with time in the composite submitted to impact with both projectiles*

Thus, as indicated in the introduction, the high performance of such a composite in terms of density and elasticity in yarn directions allows a fast dissipation of kinetic energy as strain waves over a large area of the plate first. These strains are related to intense stresses into the plies in their main directions and at the interfaces between the plies. This is probably responsible for a part of the delamination of the composite. Also, during its penetration and arrest, the projectile perforates a few layers, probably by transverse shearing and transversally deflects the non-perforated layers of the composite laminate. This last effect is supposed to increase the delamination and contributes to the kinetic energy absorption. Also, it is responsible for the formation of the cone at the bottom of the plate.

3.2 Post-mortem analysis of composite plates

The post-mortem examination of the impacted composite plates was performed. A transparent through the thickness view of the front and bottom faces of the impacted plates with both projectiles (Figs. 7 and 8) indicates that the generated holes are similar (Figs. 7(a) and 8(a)) while both projectiles have different diameters. It is probably due to local retraction of the material at the border of the holes. On the other hand, Projectile 2 generated much more damages than Projectile 1 as the dark region indicating the presence of delamination is bigger (Figs. 7(b) and 8(b)), reaching even a boundary of the plate. It can be noted that the damages of both composite plates can be separated into three main regions. The smallest and diamond-like one is due to a complete delamination and separation between the plies of the laminate (internal dashed circle on Figs. 7(b) and 8(b)). It is also the closest region to the impact. In this region, a cone was developed during the impact. The second and intermediate region corresponds to the delamination of the composite plies but a contact remains between them (external dashed circle on Figs. 7(b) and 8(b)). Finally, far from the impact point, the composite keeps its integrity but the tensile stresses spreading the kinetic energy of the projectiles were responsible for plane permanent deformations of the laminate, which is visible at their boundaries. Also, the plate impacted with Projectile 2 presents clear lateral retraction at the boundaries and most of the filaments were apparently bent during the impact.

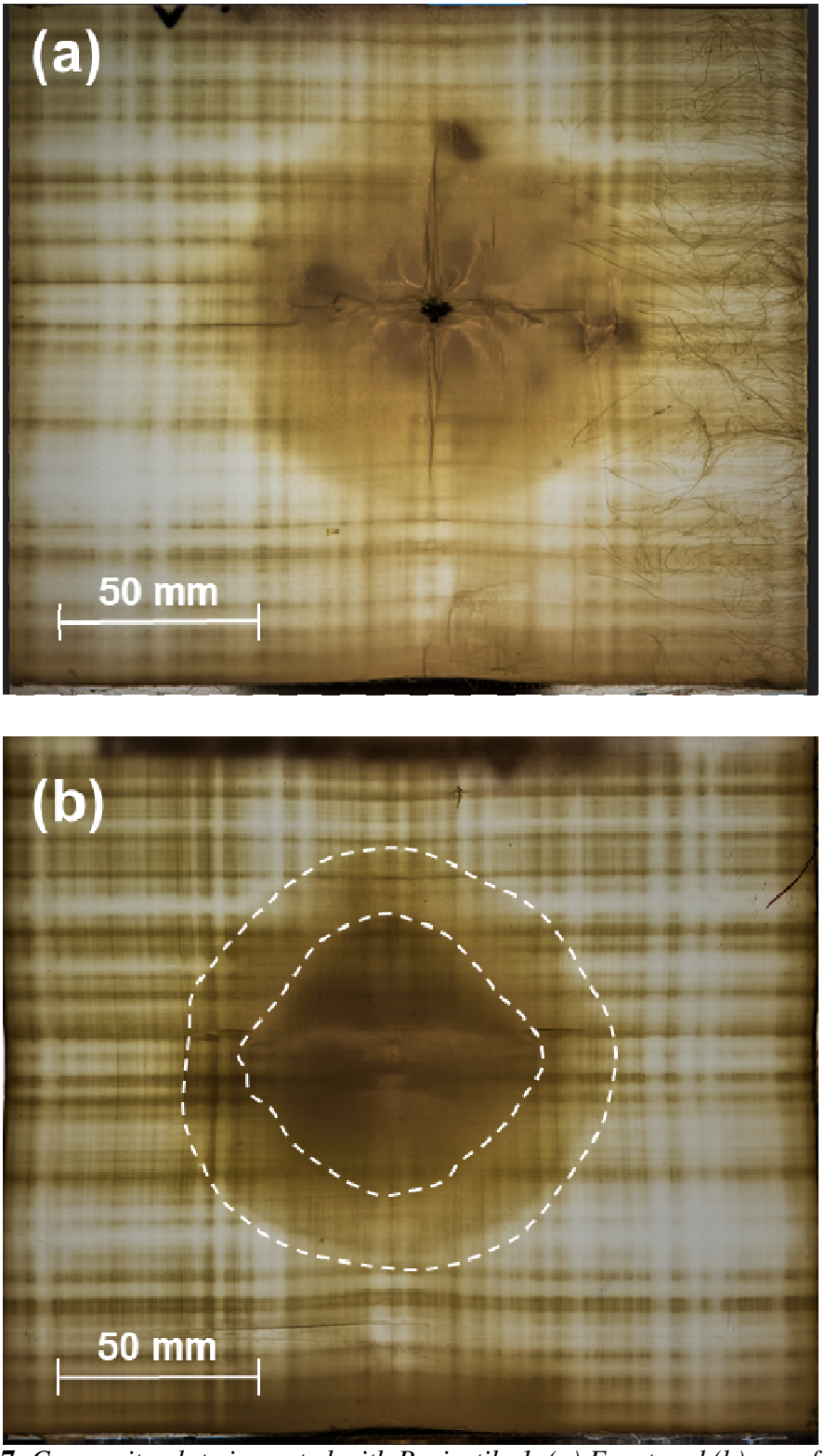

Fig. 7. *Composite plate impacted with Projectile 1. (a) Front and (b) rear faces*

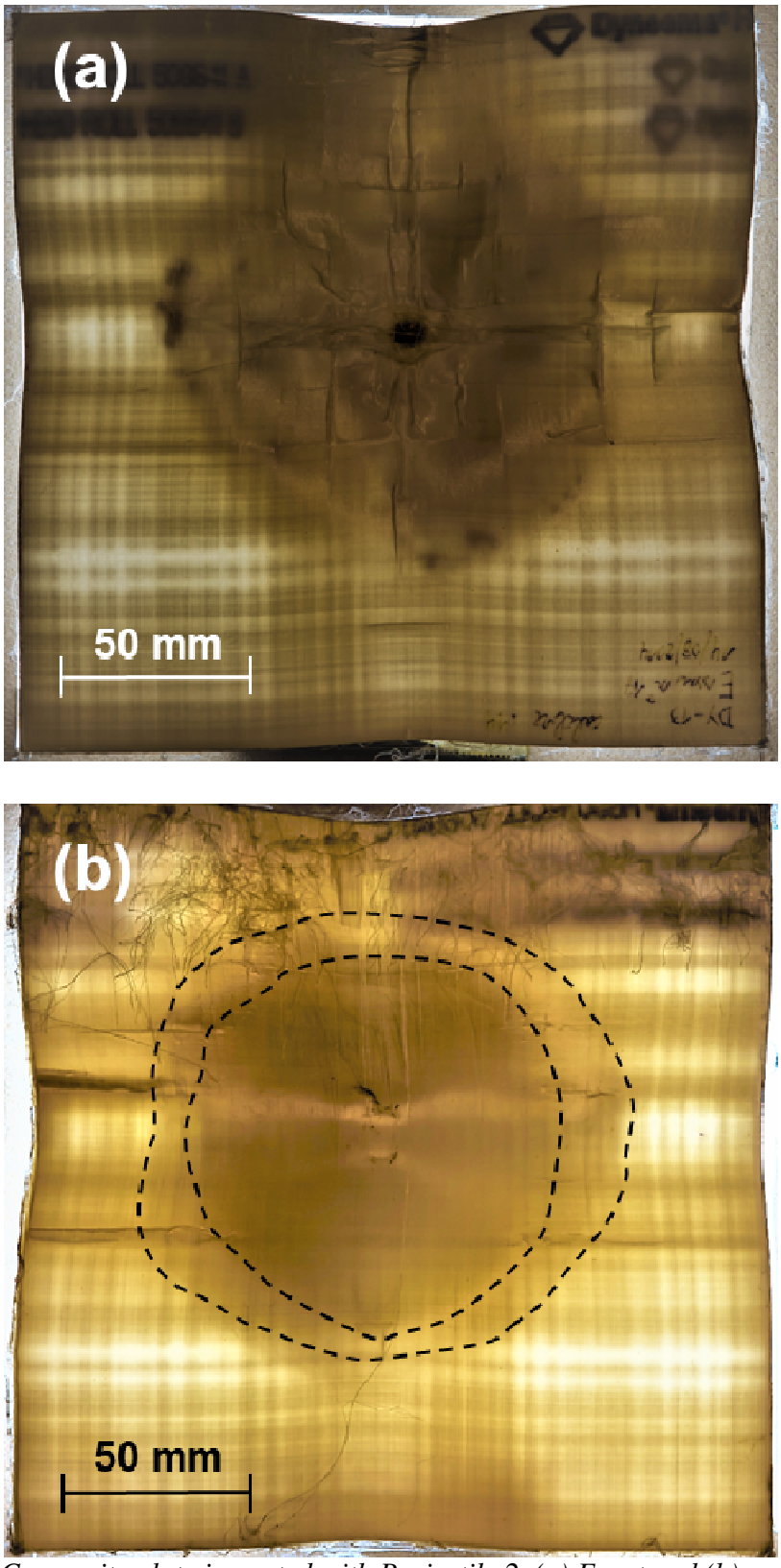

Fig. 8. *Composite plate impacted with Projectile 2. (a) Front and (b) rear faces*

To perform a cross-sectional analysis of the damaged laminates, the two plates (impacted by projectiles 1 and 2) were carefully cut with a micro bandsaw Proxxon MBS 220/E with a coarsed-toothed (14 TPI) blade for aluminium and plastic.

The cross-sectional analysis of the plate impacted with Projectile 1 (Fig. 9) indicates three types of damages. Firstly, the front face layers of the laminate are perforated, probably by shearing. It could be noted that these perforated layers recovered almost totally their initial position, probably by elasticity. Secondly, there is apparently just one delamination between the perforated and intact layers of the laminate, stopping the projectiles. Finally, a permanent deflection of the intact layers, behind the projectile, can be observed. The latter can probably be explained by at least a partial plastic behaviour of such a material.

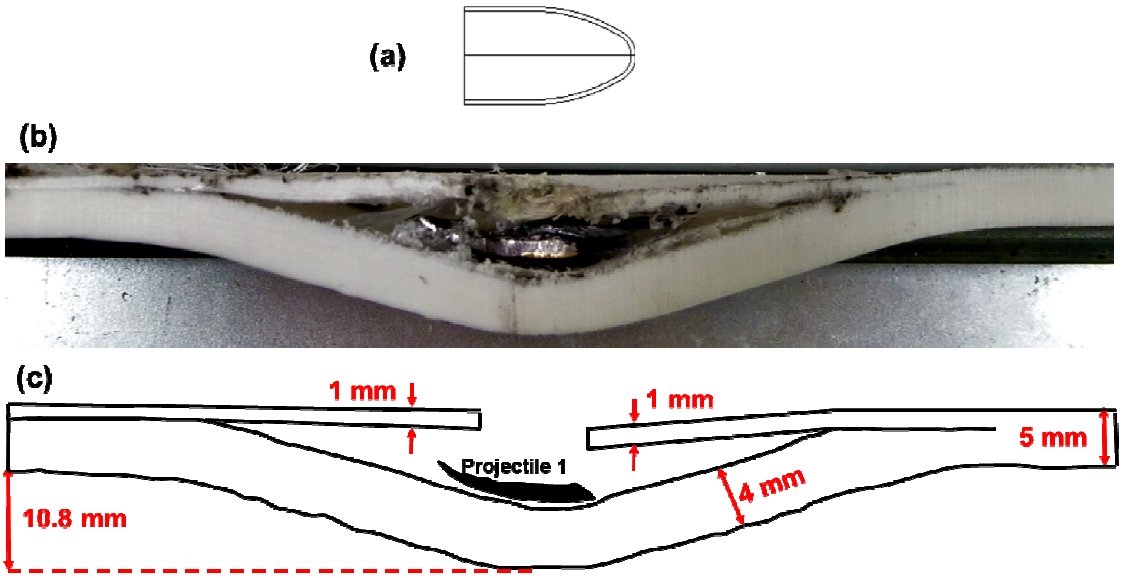

Fig. 9. *(a) Sketch of Projectile 1, (b) cross-sectional view of damages of the plate and (c) schematic description of damages of the plate*

In the case of the plate impacted with Projectile 2 (Fig. 10), the same damage mechanisms as for Projectile 1 can be observed. Nevertheless, the global deflection of the plate is clearly more important. The front perforated layers exhibit a much more important permanent deflection than in the impact case with Projectile 1. Finally, the most important difference between the two studied impact cases, is probably the presence of multiple interlaminar delaminations between the layers behind Projectile 2, on the left side of the impacted region. Also, it can be observed three complete separations between layers of the laminate in this region. As this projectile is large with a flat front face, it could be assumed that it generates a powerful shock pressure wave propagating through the thickness of the composite at the beginning of impact. Very often, such a wave rebounds at the bottom of the target plate into a tensile wave. In the case of more brittle targets, it is well known to be responsible for spalling. For a laminate composite, delamination can probably replace the spalling. Finally, it can also be observed that the final position of the projectile is slightly inclined. While it is difficult to conclude about

such an asymmetry, it can possibly be explained by the flat nose shape of this projectile or a slight shift of the real impact region from the centre of the plate.

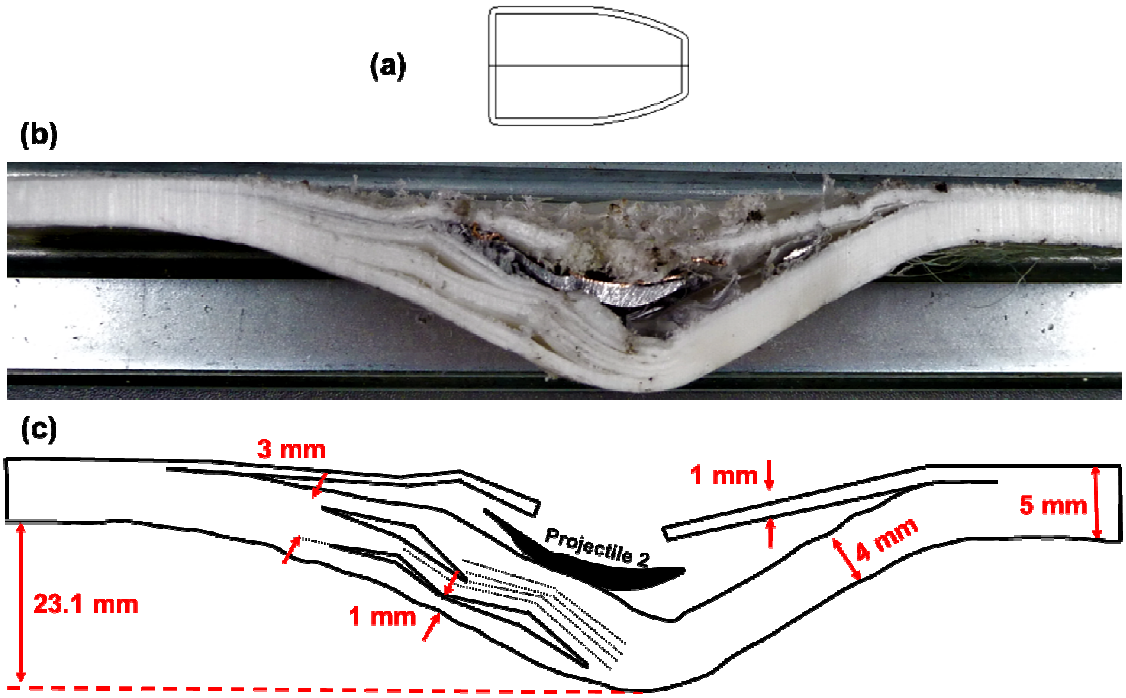

Fig. 10. *(a) Sketch of Projectile 2, (b) cross-sectional view of damages of the plate and (c) schematic description of damages of the plate*

Concerning the delamination observed in both composite plates, it is difficult to determine if it concerns more the interfaces between plies or sub-layers constituting the plies. Indeed, it was not possible to distinguish these two different interfaces. Nevertheless, it is supposed that both types of interfaces probably play a role in the delamination process but further investigations should be conducted to better understand their respective influences.

It can also be observed that the thickness or number of perforated plies seem to be similar with both projectiles. The numerical simulations seem to confirm this fact (Fig. 11). Indeed, according to the models, 14 layers are perforated by Projectile 1 while 16 layers are perforated by Projectile 2. Also, it can be noted that the depth of the penetration cone is more than 2 times greater with Projectile 2 than with Projectile 1. The greater value obtained with Projectile 2 indicates that more energy is dissipated during the impact in this case. The maximum height of the cone evaluated with the model is really in good accordance in the case of Projectile 1. However, in the case of Projectile 2, the simulation slightly underestimates this value, probably because of the pure orthotropic elastic nature of the proposed constitutive equation for the laminate. Only elastic deformation, inter-ply delamination and failure based on a yield stress criterion (numerical erosion) are implicated in the present simulations. Therefore, a more complete orthotropic elasto-plastic constitutive equation for the composite could probably improve the prediction of the model. Indeed, more complete orthotropic models taking into account of plasticity

coupled with damages exist. Nevertheless, in the case of DYNEEMA® HB80, further mechanical studies should be performed to get mechanical parameters related to plasticity and damage for feeding such complex orthotropic constitutive equations. For example, based on an extensive experimental procedure on DYNEEMA® HB26 plates, Lässig et al. [5,11,13] deduced a complex non-linear orthotropic behaviour, including a shock equation of state. Conducted on DYNEEMA® HB80 samples, such an approach would give access to more precise models for this particular composite under ballistic impact conditions.

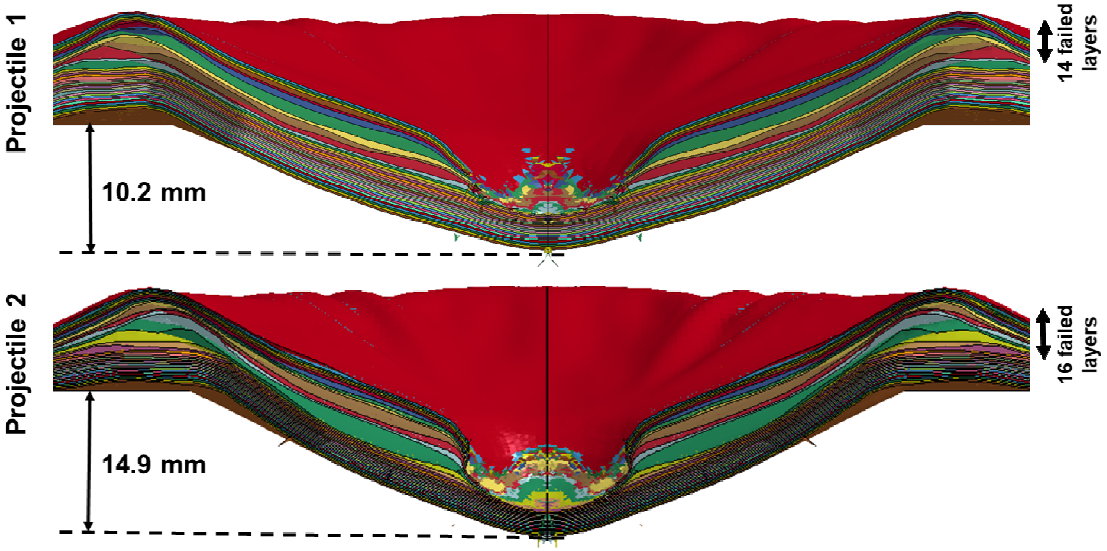

Fig. 11. *Numerically assessed damages through the thickness of the composite armour plates for both projectiles*

Finally, when comparing Figs. 7(b) and 8(b) to the final aspect of the simulated plates (Figs. 12 and 13), it can be observed that the three different damage regions are properly predicted by the numerical models. Also, the dimensions of these different damage regions are very well estimated by the models.

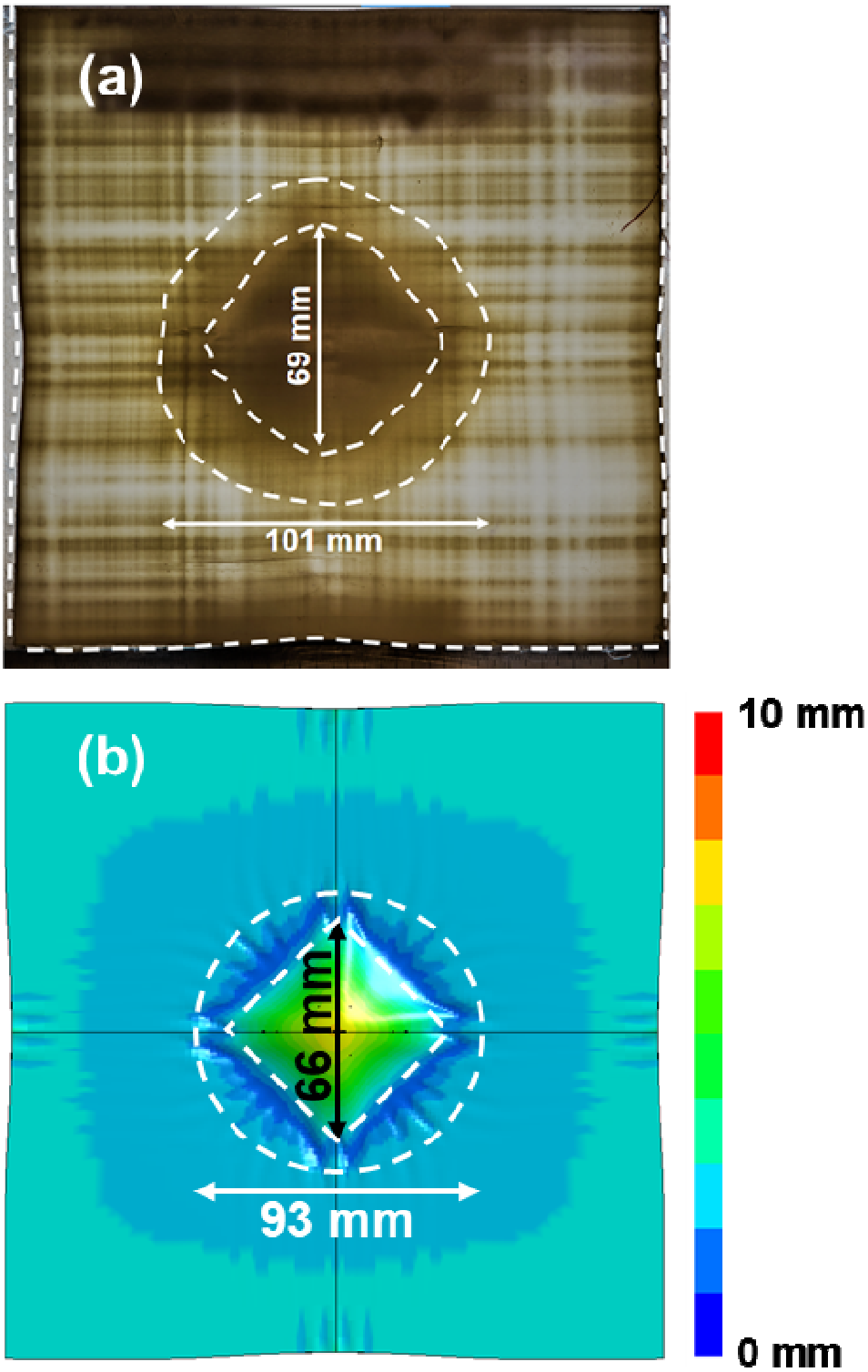

Fig. 12. (a) *Rear surface of the damaged composite sample and (b) result of the corresponding simulation in terms of out-of-plane displacement (Projectile 1)*

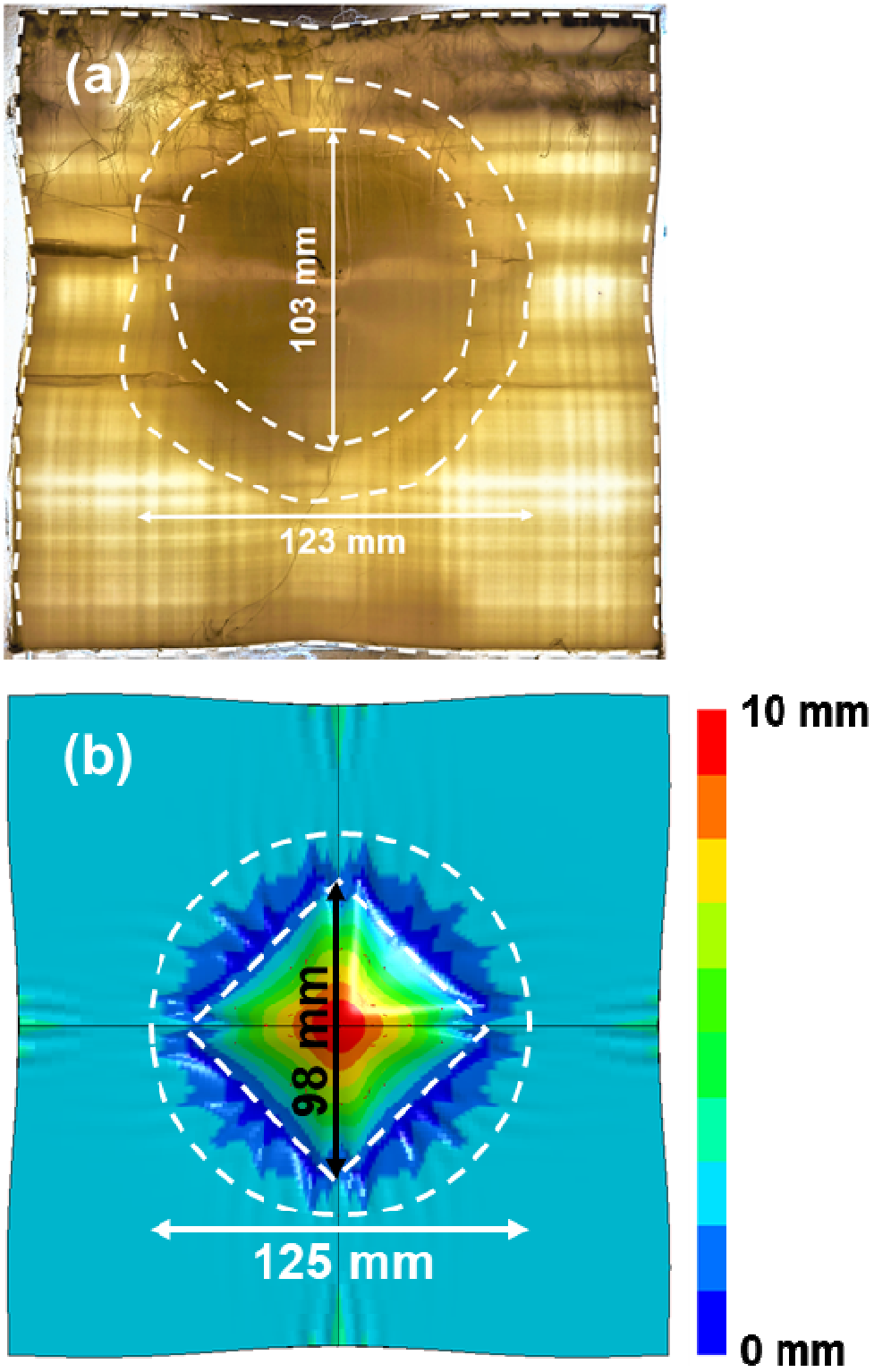

Fig. 13. (a) *Rear surface of the damaged composite sample and (b) result of the corresponding simulation in terms of out-of-plane displacement (Projectile 2)*

5. Conclusion

The structure of plates of DYNEEMA® HB80 were examined in details to model this specific material with a macroscopic approach and a suitable constitutive equation. A few numbers of samples were impacted by two different bi-metallic projectiles. All the projectiles were stopped by the composite armour.

The kinetic energy of the projectiles was spread by different damage mechanisms. Post-mortem examination of the plates indicated that the main damage mechanisms are fibre breaking, delamination and permanent backface deflection. Also, Projectile 2 had systematically an inclined position in the plate while Projectile 1 keeps a righter position. It is supposed that this effect results from the head shape of Projectile 2, or a slight shift of the impact place from the centre of the plate. Moreover, Projectile 2 seems to be responsible for a spalling-like process of the armour whose mechanism is based on a great amount of delamination.

As the penetration process is not visible, assessment of the damages in real-time was performed with numerical simulations. From the post-mortem inspection of the plates, it was observed a good correlation between the tests and models in terms of permanent damages.

The simulations indicated that Projectile 2 needs a greater time to lose its kinetic energy, thus, to be stopped than Projectile 1. As the penetration process occurs, the first plies of the laminate are perforated before the residual plies act as a net to stop the projectiles. According to the models, the kinetic energy of the projectile is mainly dissipated by tensile stresses distribution in the main directions of the composite.

Finally, further mechanical studies should be performed on DYNEEMA® HB80 construction. Indeed, more complete knowledge about its behaviour in terms of plasticity, damage criteria, inter-plies and sub-layers interfaces mechanical response would give access to more refined simulations of the behaviour of this specific material under ballistic impacts.

Acknowledgement

This research was conducted with the support of the Royal Military Academy's Dynamic Material Behaviour and Security Applications research department, which provided valuable support for the experimental and numerical work carried out in the framework of the aforementioned study. Also, a sincere thank you to Mr Messaoud CHAYANI, from Lille University Graduate School of Engineers, Department of Foreign Languages, for his diligent proofreading of this paper.

References

[1] Tan VBC, Lim CT, Cheong CH. Perforation of high-strength fabric by projectiles of different geometry. Int J Impact Eng 2003;28:207–222. https://doi.org/10.1016/S0734-743X(02)00055-6.

[2] Bhatnagar A. Lightweight ballistic composites. Military and law-enforcement applications. Whoodhead Publishing in Materials, 2006.

[3] O'Masta MR, Deshpande VS, Wadley HNG. Mechanisms of projectile penetration in Dyneema® encapsulated aluminum structures. Int J Impact Eng2014;74:16-35. https://doi.org/10.1016/j.ijimpeng.2014.02.002.

[4] Van der Werff H, Heisserer U. High performance ballistic fibres: Ultra-High Molecular Weight Polyethylene (UHMWPE). Advanced Fibrous Composite Materials for Ballistic Protection, Chapter 3, 71-107, 2016. https://doi.org/10.1016/B978-1-78242-461-1.00003-0.

[5] Lässig TR, May M, Heisserer U, Riedel W, Bagusat F, Van der Werff H, Hiermaier SJ. Effect of consolidation pressure on the impact behavior of UHMWPE composites. Compos Part B Eng 2018;147:47–55. https://doi.org/10.1016/j.compositesb.2018.04.030.

[6] Van der Werff H, Heisserer U, Lässig T, Riedel W. New protection levels of UHMWPE armour: From a hydrocode model of HB26 to new generation Dyneema® for armour applications. Proceedings of Personal Armour Systems Symposium (PASS2014), Cambridge, UK, 2014.

[7] Cunnif PM. Dimensional parameters for optimization of textile-based body armor systems. Proceedings of the 18th International Symposium of Ballistics, San Antonio, TX, USA, 15-19 November 1999.

[8] Austin S, Brown AD, Escobedo JP, Wang H, Kleine H, Hazell PJ. The high-velocity impact of Dyneema® and Spectra® laminates: implementation of a simple thermal softening model. Procedia Eng 2017;204:51–58. https://doi.org/10.1016/j.proeng.2017.09.725.

[9] Phoenix SL, Heisserer U, Van der Werff H, Van der Jagt-Deutekom M. Modeling and Experiments on ballistic impact into UHMWPE yarn using flat and saddle-nosed projectiles. Fibers 2017;5(1):8. https://doi.org/10.3390/fib5010008.

[10] Zhang D, Sun Y, Chen L, Zhang S, Pan N. Influence of fabric structure and thickness on the ballistic impact behavior of Ultrahigh molecular weight polyethylene composite laminate. Mater Design 2014;54:315-322. https://doi.org/10.1016/j.matdes.2013.08.074.

[11] Lässig T, Riedel W, Heisserer U, Van der Werff H, May M, Hiermaier S. Numerical sensitivity studies of a UHMWPE composite for ballistic protection. WIT Transactions on The Built Environment 2014;141:371-381. https://doi.org/10.2495/SUSI140321.

[12] Karthikeyan K, Russell BP. Polyethylene ballistic laminates: Failure mechanics and interface effect. Mater Design 2014;63:115–125. https://doi.org/10.1016/j.matdes.2014.05.069.

[13] Lässig T., Nguyen L., May M., Riedel W., Heisserer U., Van der Werff H., Hiermaier S., "A non-linear orthotropic hydrocode model for ultra-high molecular

weight polyethylene in impact simulations", Int J Impact Eng, 75, 110-122, 2015. https://doi.org/10.1016/j.ijimpeng.2014.07.004.
[14] Grunwald C, Lässig TR, Van der Werff H, Heisserer U. Numerical sensitivity of ballistic impact on UHMWPE composites. Proceedings of the 6th International Conference on Design and Analysis of Protective Structures (DAPS 2017), Melbourne, Australia, 2017.
[15] Hazzard MK, Trask RS, Heisserer U, Van Der Kamp M, Hallett SR. Finite element modelling of Dyneema® composites: from quasi-static rates to ballistic impact. Compos Part A Appl Sci Manuf 2018;115:31-45. https://doi.org/10.1016/j.compositesa.2018.09.005.
[16] Chocron S, King N, Bigger R, Walker JD, Heisserer U, Van der Werff H. Impacts and waves in Dyneema® strips and laminates. J Appl Mech 2013;80(3):031806. https://doi.org/10.1115/1.4023349.
[17] Zhang TG, Satapathy SS, Vargas-Gonzalez LR, Walsh SM. Ballistic impact response of Ultra-High-Molecular-Weight Polyethylene (UHMWPE). Compos Struct 2015;133:191-201. https://doi.org/10.1016/j.compstruct.2015.06.081.
[18] Chocron S, Zaera R, Walker J, Brill A, Kositski R, Havazelet D, Heisserer U, Van der Werff H. Transitioning a unidirectional composite computer model from mesoscale to continuum. EPJ Web of Conferences 2015;94:04048. https://doi.org/10.1051/epjconf/20159404048.
[19] Hallquist JO. LS-DYNA® theory manual. Livermore Software Technology Corporation (LSTC), 2006.
[20] Gilson L, Rabet L, Imad A, Coghe F. Experimental and numerical assessment of non-penetrating impacts on a composite protection and ballistic gelatine. Int J Impact Eng 2020;136:103417. https://doi.org/10.1016/j.ijimpeng.2019.103417.
[21] Heisserer U. Tensile properties of Dyneema HB plies (HB2, HB26, HB50, HB80). Technical report, DSM-Dyneema, 2011.
[22] Azevedo A, Coghe F, Miranda Vicario A, Texeira-Diaz F. Modeling the ballistic behavior of DYNEEMA® HB26 and HB80 using LS-DYNA. Proceedings of the LWAG Symposium and Industry Focus Day, Brussels, Belgium, 2013.
[23] Zhang TG, Satapathy SS, Vargas-Gonzalez LR, Walsh SM. Effect of boundary conditions on the back face deformations of flat UHMWPE panels. Proceedings of the Composites and Advanced Materials Expo (CAMX) conference, Orlando, Florida, USA, 2014.
[24] Gilson L, Rabet L, Imad A, Kakogiannis D, Coghe F. Development of a numerical model for the ballistic penetration of Fackler gelatine by small calibre projectiles. Eur Phys J 2016;225(2):375–384. https://doi.org/10.1140/epjst/e2016-02640-9.
[25] Gilson L, "Etude du comportement mécanique des multi-matériaux soumis à un impact balistique : approches expérimentale et numérique", PhD thesis, Royal Military Academy & Université de Lille 1 Sciences et Technologies, 2017.